

CrossMark
click for updates

Research

Cite this article: Lankheet MJ, Stoffers T, van Leeuwen JL, Pollux BJA. 2016 Acquired versus innate prey capturing skills in super-precocial live-bearing fish. *Proc. R. Soc. B* **283**:

20160972.

<http://dx.doi.org/10.1098/rspb.2016.0972>

Received: 3 May 2016

Accepted: 21 June 2016

Subject Areas:behaviour, biomechanics,
developmental biology**Keywords:**live-bearing fish, prey capture behaviour,
innate motor patterns, postnatal development,
visuo-motor coordination, pectoral fins**Author for correspondence:**

Martin J. Lankheet

e-mail: martin.lankheet@wur.nlElectronic supplementary material is available
at <http://dx.doi.org/10.1098/rspb.2016.0972> or
via <http://rspb.royalsocietypublishing.org>.Acquired versus innate prey capturing
skills in super-precocial live-bearing fishMartin J. Lankheet, Twan Stoffers, Johan L. van Leeuwen
and Bart J. A. PolluxExperimental Zoology Group, Department of Animal Sciences, Wageningen University, Wageningen,
The Netherlands

Live-bearing fish start hunting for mobile prey within hours after birth, an example of extreme precociality. Because prenatal, *in utero*, development of this behaviour is constrained by the lack of free-swimming sensory-motor interactions, immediate success after birth depends on innate, evolutionarily acquired patterns. Optimal performance however requires flexible adjustment to an unpredictable environment. To distinguish innate from postnatally developing patterns we analysed over 2000 prey capture events for 28 metallic livebearers (*Girardinus metallicus*; Poeciliidae), during their first 3 days after birth. We show that the use of synchronous pectoral fin beats for final acceleration and ingestion is fixed and presumably innate. It allows for direct, symmetrical control of swimming speed and direction, while avoiding head yaw. Eye movements and body curvatures, however, change considerably in the first few days, showing that eye-tail coordination requires postnatal development. The results show how successful prey captures for newborn, live-bearing fish are based on a combination of fixed motor programmes and rapid, postnatal development.

1. Introduction

In mammals and birds, the altricial–precocial spectrum is used to indicate the functional independence of offspring at birth [1]. Altricial young (e.g. primates and passerines) completely depend on their parents for feeding and protection. By contrast, precocial young (e.g. ungulates and galliform birds) have well-developed locomotor skills at birth, allowing them to forage independently. Super-precocial animals occupy the most extreme end of this spectrum, with neonates that are capable of highly complex behaviours (e.g. blue wildebeest, *Connochaetes taurinus* and megapode birds [1–3]).

An altricial–precocial spectrum also exists in fish [4]. Oviparous (egg-laying) fishes are altricial, lacking well-developed visual and locomotor systems at hatching. Hatched larvae rely on endogenous nutrient reserves in their yolk sac for several days or weeks, depending on the species. By contrast, viviparous (live-bearing) fishes are precocial, producing large, well-developed young that lack a yolk sac at birth and instead rely on active exogenous feeding after birth [5,6]. Live-bearing toothcarps of the family Poeciliidae are an example of extreme precociality, having large, well-developed neonates that catch pelagic, free-swimming prey within hours after birth.

Catching mobile prey is a particularly complex, visually guided motor task that requires adequate, calibrated interactions of visual and locomotor skills [7–14]. To optimize chances for survival these skills must either be present at birth, or quickly develop after birth. Although the ontogenetic development of sensory-motor skills has been studied extensively in the egg-laying zebrafish [15–17], it remains unclear how live-bearing fish develop these skills. They have an extended period of initial *in utero* development and are born in an advanced juvenile stage. This development, however, takes place in the absence of normal visual input and motor output and therefore lacks appropriate feedback required for visuo-motor learning [12,18,19]. Nevertheless, neonates catch

prey almost immediately after birth, suggesting that part of their hunting skills must be innate.

Here, we examine how neonates of the super-precocial live-bearing fish *Girardinus metallicus* (Poeciliidae) manage to catch prey and to what extent prey-capturing skills are present at birth, or develop postnatally. We analysed more than 2000 high-speed videos of prey-capturing events during the first 3 days after birth. By analysing and comparing body movements, pectoral fin movements and eye movements, we identify components of their hunting behaviour that remain unaltered, and hence are presumably innate, and components that require postnatal development.

2. Material and methods

(a) Experimental protocol

We isolated individual fish in Petri dishes (33.1 mm diameter) early in the morning after the night they were born. To record prey capture events on film, the Petri dish with the fish was transferred to an experimental set-up and fish were individually fed recently hatched *Artemia* nauplii, one at a time. *Artemia* swam irregularly, at speeds of about 4–10 mm s⁻¹ on average. All prey capture events were recorded on video (see the electronic supplementary material, movies S1 and S2). Recordings continued until the fish were satiated. To prevent acute stress due to large changes in luminance level, newborn fish were allowed to slowly adjust to the light regime in the experimental set-up before the first recording in a session. Hereto, lighting was gradually increased from 0 to 100% (7000 lux) in 10 min. The procedure was conducted twice daily for each fish on day 1, 2 and 3 after birth. The fish did not receive any additional food during these 3 days. Outside the experimental set-up they were held at the normal 12 L : 12 D cycle, in a stove at 24°C.

(b) Recordings

Prey capture events were filmed with a Mikrotрон EoSens MC1362 high-speed camera at 500 frames s⁻¹, at a spatial resolution of 31 pix mm⁻¹ and 1 ms shutter time. The fish were filmed from the dorsal side against an array of LEDs behind a white, translucent plate. In addition, we used a circular array of LEDs behind a through-projection screen for equal lateral illumination from all sides. Lighting from below and from the sides was optimized to obtain maximal contrast between body and background, between the eyes and the rest of the body, and prey relative to the background. The Petri dish containing the fish was raised about 2 cm above the bottom plate to minimize temperature fluctuations. Filming from the ventral side was avoided because it led to optical effects of the fish eyes that prevented proper determination of eye orientation.

To record prey capture events, we used a circular frame buffer of 4 s duration. After starting a session, a single prey was introduced in the centre of the Petri dish. The recording was stopped after the prey was successfully captured. When perfectly timed this would give a thousand frames before and after the catch. In practice, however, the timing was quite variable causing losses before and after prey encounter. In addition, only scenes in which the fish was not located close to the side of the dish were useful for analysis. For each sequence, a suitable range of frames around prey ingestion was selected, and the moment of ingestion, quantified as the last frame in which the prey was still visible outside the fish, was marked as a reference point in time ($t = 0$).

(c) Data analysis

We used custom software developed in MATLAB® (R2013b, The MathWorks™ Inc., Natick, MA, USA), including the image

analysis toolbox, to automatically extract all relevant parameters from the movies. These parameters include kinematic data such as swimming velocity, body curvatures and pectoral fin movements, as well as parameters specifically related to the visually guided behaviour. The latter include eye orientations, prey location, and viewing and swimming directions relative to the prey. Electronic supplementary material, figure S1, provides an illustration and definition of the list of parameters. In addition, they are illustrated and explained in figure 2, where we discuss an example of a capture event.

(i) Eye orientations

Although larval fish may be very sensitive to water flow [20] and prey might be detected by the lateral line system, in the capture events that we studied, prey detection and approach was largely visually driven. When presenting the *Artemia* in a transparent, invisible, polyethylene tube (refractive index equal to that of water), the fish still showed qualitatively the same prey attack behaviour. Electronic supplementary material, figure S2, explains how eye orientations were obtained from the images. The eyes were found using an adaptive threshold, and selecting the two objects furthest away from the centroid of the silhouette of the fish. A 'cyclopean' eye was defined as the midpoint in between the centroids of the eyes. It served as a general reference point for further calculations, and for defining movements of the fish. Eye orientations were calculated as the orientations of the 'straight' corneal contrast border between the eyes and the surroundings. In this way, eye orientation was insensitive to variations in grey levels or contrast differences between eyes and body due to differences in body pigmentation.

Eye orientations were quantified by a vergence angle and a version angle [21]. Vergence describes the angle between the two eyes (see the electronic supplementary material, figure S1; figure 2*h*). Zero vergence indicates parallel eyes, facing laterally and an increase in vergence angle corresponds to an inward rotation of the eyes, as required to view objects nearby. The version angle was defined as the mean orientation of the two eyes relative to the midline of the head (figure 2*i*). It describes the viewing direction in head-centred coordinates. The fixation error was defined as the mismatch between the version angle (i.e. viewing direction) and the direction of the centroid of the *Artemia* relative to the cyclopean eye, given in degrees. Zero fixation error corresponds to symmetrical viewing of the prey with left and right eye.

(ii) Body curvature and head orientation

To extract swimming movements of body and tail, we used a set of filters to extract the silhouette of the fish, excluding the fins. The midline of the silhouette was calculated based on the maxima in the 'distance transform'. The central axis was parameterized at fixed distance steps relative to the cyclopean eye, which was the first point on the central axis (see the electronic supplementary material, figure S1). The orientation of the head was calculated as a straight line fitted to the anterior 1/8th of the total axis. Curvature of the body axis was obtained by differentiation of a polynomial fitted to the axis orientation and is given in degrees per millimetre. To discard differences in axis length (owing to differences in visibility of the tail fin), we adjusted all axes to the minimal length in a movie. To study curvatures as a function of time (e.g. figures 2*c* and 3*b*), we averaged the absolute values of curvatures along the axis.

(iii) Prey location

To identify the *Artemia* and distinguish it from possible dirt particles, we determined its location by first finding an appropriate object closest to the tip of the snout, just before a strike. This object was then tracked back to the beginning of the movie. The distance to the *Artemia* was defined relative to the cyclopean eye.

To quantify the accuracy of approaching the prey, we calculated the aim error (figure 2*d* and electronic supplementary material, figure S4) as the minimal distance between the *Artemia* and the midline of the head of the fish (see the electronic supplementary material, figure S1). It is more stable at short distances than an angular mismatch.

(iv) Pectoral fins

Pectoral fins were detected using a standard edge detection filter restricted to a maximum distance from the centre of gravity of the silhouette. By subtracting anything coinciding with the silhouette of the fish, we isolated objects corresponding to the fins (see the electronic supplementary material, figure S1). The projected surface area for the left and right pectoral fin (figure 2*g*) was determined as an indication for the rotation of the fin relative to a horizontal plane. Abduction angles were calculated from the front-most point on a distal part of the fin relative to the insertion point of the fin (the part of the fin border that moved the least, in a head-centric coordinate system). To distinguish synchronous fin movements from alternating fin movements, we defined the angle between the two fins as the sum of their abduction angles (figure 2*f*). It changes rapidly for synchronous movements but remains relatively constant for alternating fin movements. Modulation amplitudes and frequencies for abduction angle and for projected fin area were calculated using a discrete Fourier transform (FFT) for signals of 300 ms duration, starting 360 ms before the final strike ($t = 0$). To increase the frequency resolution, the data were padded with zeros to a length of 1024 samples.

After determining parameters in separate frames, we removed 180° jumps in the data, and performed mild smoothing as a function of frame number. In this procedure, we replaced outliers by the mean value of the neighbouring points. Outliers were determined as points deviating more than five times the standard deviation of the distance between successive points from the mean of its neighbours. Smoothing was established by a 5-point, weighted moving average. Owing to the high frame rate, this filter got rid of high frequency noise in the data while minimally affecting frequency components of interest. For each parameter, we kept track of missing data points in the time sequence, to properly average the data. Missing data points could be owing to timing errors in starting and stopping the high-speed movies (resulting in either the beginning or end part missing) or due to e.g. dirt particles in the water interfering with part of the analysis.

(d) Data selections

We only included capturing events that were successful on the first attempt. This excludes failed attempts, and also removes any movies including failed attempts before a final successful attempt. By excluding failed attempts, we focus on inherent changes in prey capture behaviour, irrespective of the immediate cause of failures. Instead of analysing the variety of possible errors in prey capture, we focus on consistent changes in behaviour. Finally, we removed a small number of movies that yielded obviously erroneous data, mostly due to poor contrast between eyes and the rest of the body, preventing accurate localization of the eyes.

(e) Statistical analyses

Changes in fish length, fin abduction amplitude and frequency and projected fin area amplitude and frequency during the first 3 days after birth were tested by means of general linear mixed modelling (GLMMs) using the MIXED procedure in SAS v. 9.3 (SAS Institute Inc., Cary, NC, USA, 2010). The data from individual fish that were measured on the different days were expected to be correlated. To adequately account for this effect, models were fitted using the repeated statement with fish individual treated as the subject effect and with mother included as a

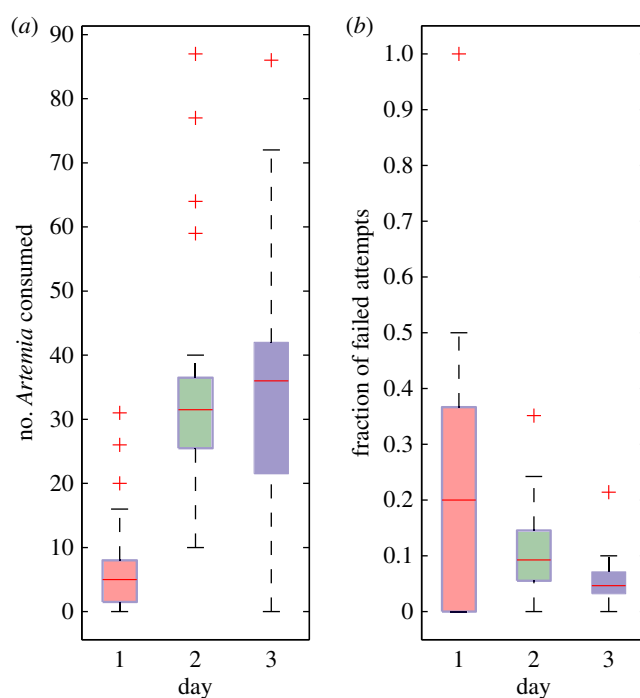


Figure 1. Statistics of feeding behaviour per fish on days 1, 2 and 3. (a) Numbers of *Artemia* consumed. (b) Fraction of failed attempts. Data were obtained for 28 fish. Boxes represent median values \pm 25 percentiles; whiskers span the range of values, excluding outliers (red crosses). On day 1, data are missing for five fish and on day 3 for six fish. (Online version in colour.)

random effect [22]. Changes in the probability of successful prey capture and total number of consumed prey, during the first 3 days were assessed by fitting GLMMs to the data using the GLIMMIX procedure in SAS v. 9.3. The probability of prey capture (a dichotomous response variable) was modelled assuming a binomial response distribution and a logit link function and the total number of consumed prey (a discrete response variable based on count data) was modelled assuming a Poisson frequency distribution and log link function. Models were fitted by including day as a repeated effect (using the residual-keyword in the random statement), individual as the subject effect and mother as a random effect [22]. To evaluate differences between days, pairwise post hoc comparisons of means were performed using a Bonferroni adjusted comparison-wise error rate of $P(\alpha/3) < 0.0167$.

For comparing response parameters across days at a specific time before the strike, we employed a Skillings–Mack test, a generalized Friedman test, using MATLAB® R2013b (MathWork™ Inc., Natick, MA, USA) [23]. The test is used to compare data with fish individual as subject effect and day as repeated effect. Hereto, we calculated the means for all recorded prey capture events as a function of time relative to the moment of the strike ($t = 0$), for each fish and for each day (see, e.g. figures 3, 4*a* and 5). Tests were performed for data averaged over a time period of 10 ms.

3. Results

The number of prey consumed per day increased significantly during the first 3 days (GLMM: $F_{2,68} = 101.56$, $p < 0.0001$; mean \pm s.d.: 8.1 ± 8.3 , 36.4 ± 18.3 and 43.0 ± 16.0 *Artemia* per fish, respectively; figure 1*a*). Pairwise post hoc comparisons show a large and highly significant increase from day 1 to day 2 ($p < 0.001$), and a moderate, significant increase from day 2 to day 3 ($p = 0.0165$). During these 3 days, the fraction of

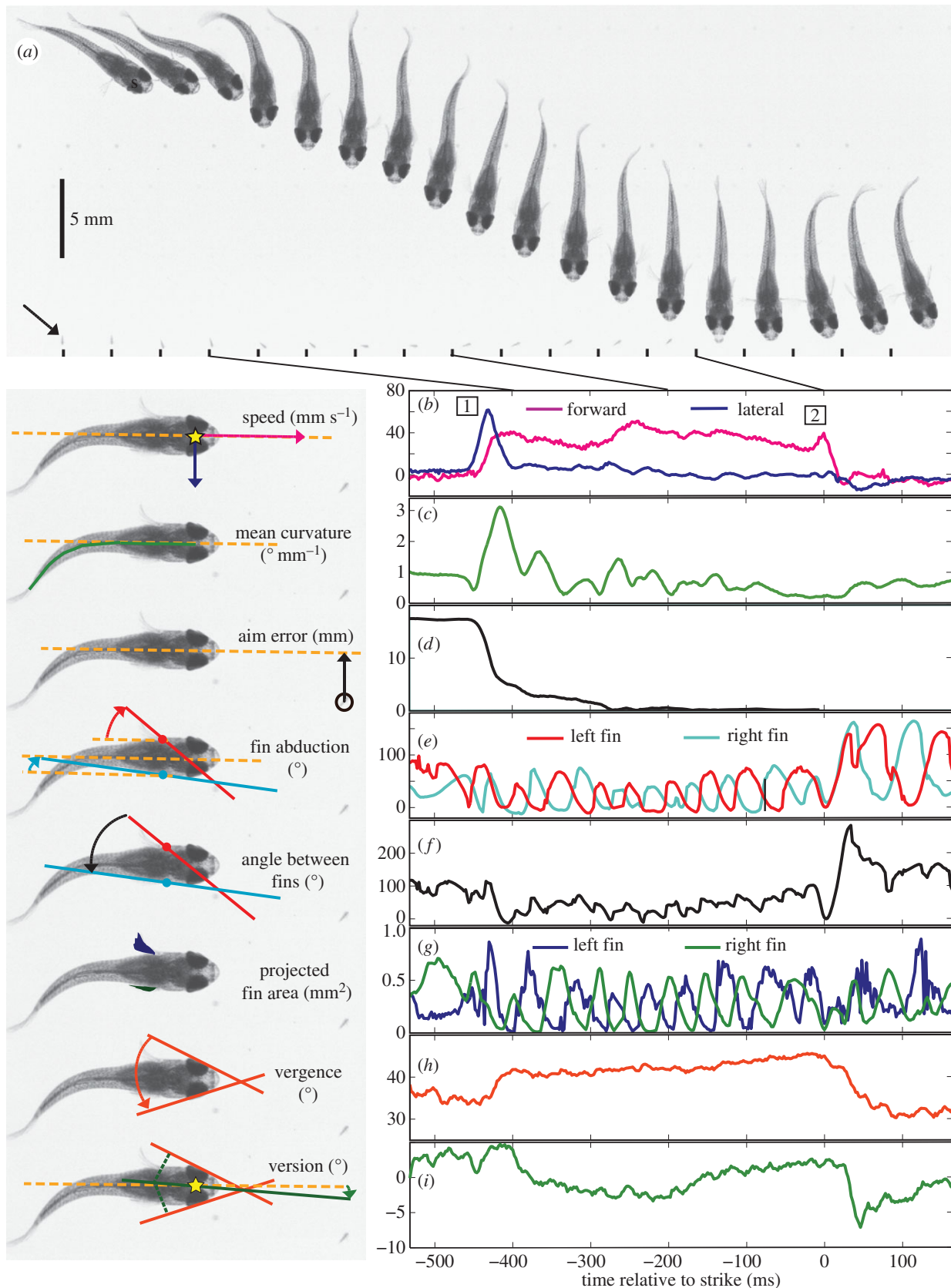


Figure 2. Example of a prey capture event for a 3-day-old fish. The fish was filmed from above at $500 \text{ frames s}^{-1}$, while capturing an *Artemia* nauplius. Panel (a) shows every 20th frame of the movie, shifted a fixed distance (indicated by the black markers) per frame to the right. The *Artemia* nauplius can be seen just above the marker at the beginning of the movie, slowly moving to the right (arrow in panel (a)). Panels (b–i) show parameters, as explained in the cartoons on the left-hand side, next to each figure. These parameters are further explained in the electronic supplementary material, figure S1. (b) Forward and lateral speed of the cyclopean eye, defined relative to the midline of the head (dashed orange line), (c) mean absolute curvature of the central axis of the fish (shown in green), (d) aim error, quantified as the shortest distance from the midline through the head to the prey (in black circle) and (e) fin abduction angles, quantified as the angle of the front edge of the fin relative to the midline. Red and blue dots indicate the insertion points of the left and right fin. (f) Angle between the two fins; (g) projected fin areas as indicators of axial fin orientation; (h) vergence angles, based on eye orientations (orange lines) orthogonal to viewing directions. Larger vergence angles correspond to increased binocular overlap; (i) version angle, defined as the deviation of the mean eye orientation, indicated by the green line, relative to the midline through the head.

failed attempts significantly decreased (GLMM: $F_{2,68} = 8.09$, $p = 0.0007$; mean \pm s.d.: 0.26 ± 0.24 , 0.09 ± 0.07 , 0.06 ± 0.06 , respectively; figure 1b), indicating an improvement in prey-capturing success. Pairwise comparisons show significant improvement from day 1 to day 2 ($p = 0.0216$), and from day 2 to day 3 ($p = 0.0244$).

Length growth during the first 3 days after birth was significant (GLMM: $F_{2,67} = 61.97$, $p < 0.0001$), but very limited; based on reconstructed body axes from recorded videos, body length increased on average 3.54% from day 1 to 2 and 2.57% from day 2 to 3 (electronic supplementary material, figure S3).

Figure 2 presents an example of a successful prey capture event, showing in detail how pectoral fins work in concert with tail and eye movements. Figure 2a shows stills from a movie sequence at 40 ms time intervals. The prey is marked by the arrow and is ingested in the fifth image from the right, at time $t = 0$. Once the prey is detected, the fish converges its eyes, executes several tail strokes to align itself and to approach the prey. Figure 2b–i show the parameters extracted from the images as a function of time. Each parameter is illustrated by the cartoon on the left, and is further explained in the electronic supplementary material, figure S1. Swimming velocity rises steeply during the initial turn (label '1' in figure 1b). It starts with an initial peak in lateral speed and is followed by a forward acceleration. During the final approach, lateral speed is minimal and forward speed slowly decreases towards the moment of the strike. Just before prey intake at $t = 0$, the fish briefly accelerates (label '2' in figure 1b), followed by a brake to standstill. Notably, the speed changes during and after the strike are not driven by tail movements, as illustrated by the low mean body curvature (figure 1c). The acceleration and deceleration around $t = 0$ result from a striking change in use of the pectoral fins, without affecting the aim error (figure 1d). During the approach, the fish makes alternating pectoral fin strokes as illustrated by counter-phase modulated fin abductions (figure 1e). Just before prey intake the pattern changes abruptly to a simultaneous, full adduction followed by a large-amplitude, synchronous abduction. This change in fin coordination is illustrated by the angle between the fins (figure 1f). It gradually increases from about 50° to 90° during approach and shows a large, fast transient at the time of ingestion, which is due to large synchronous changes in abduction angle. Rhythmic modulation of fin abductions are accompanied by similar modulations of projected fin areas, but during the synchronous fin movements, the projected fin areas are small, indicating that the fins are held in a nearly vertical plane (figure 1g). Hence, these synchronous movements may cause a large forward thrust just before prey intake, followed by a strong backwards thrust. Visual guidance of the approach is apparent from the pattern of eye movements. Upon engaging in pursuit, the fish converges its eyes, increasing its binocular visual field (figure 1h). During the approach, vergence angles gradually increase until the final strike, and then quickly drop. Version angles (figure 1i) during the approach were small and did not covary with the head orientation relative to the prey. This corresponds to an approach strategy in which the fish reduces its aim error (figure 1d) while keeping its eyes on average in a straight-ahead orientation.

To determine which components of the prey capture technique are fixed and which components show substantial changes, we compare patterns on day 1, 2 and 3 after birth. Hereto, we analysed 146 captures on day 1, 851 for day 2 and

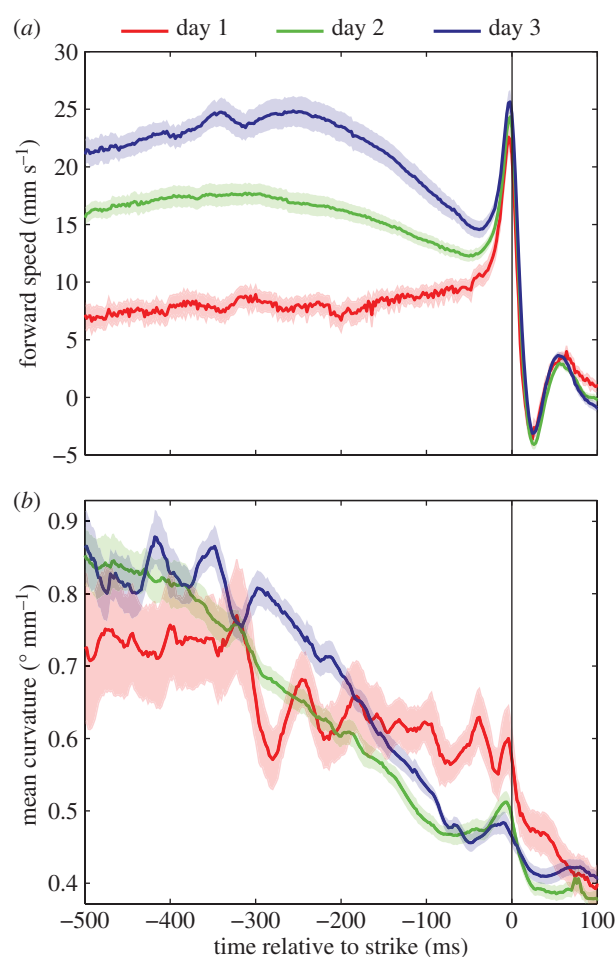


Figure 3. Mean forward speed and body curvatures during prey capture events on the day of birth (day 1) and the next 2 days (days 2 and 3). All capture events were aligned to the moment the prey disappears into the mouth ($t = 0$). For each fish and each day, all capture events were averaged, and the curves show the mean of these values for the different fish. Confidence intervals correspond to ± 1 s.e.m. Data were collected for 28 fish; on day 1 measurements are missing for five fish and on day 3 for six fish. (a) Mean forward speed of the cyclopean eye as defined in figure 1c and electronic supplementary material, figure S1. (b) Mean curvature of the central axis.

875 for day 3 and averaged the data for each individual fish. One of the striking changes was a large increase in the initial approach speed. This is illustrated in figure 3, which shows the mean value across individuals for the 3 days, and the corresponding standard errors as confidence intervals. Data for individual fish are shown in the electronic supplementary material, figure S4 and support consistency of the results, especially for day 2 and day 3. For 1-day-old fish, the forward speed was on average rather low (about $7\text{--}9 \text{ mm s}^{-1}$). For days 2 and 3, speeds were much higher during the initial approach, reaching on average about 17 mm s^{-1} at day 2 and about 24 mm s^{-1} at day 3. For day 2 and 3, average forward speeds gradually decline during the last 250 ms before the strike. The speed differences between days were highly significant. At 300 ms before the strike, for example, both groupwise and pairwise comparisons yielded p -values smaller than 0.001 (Skillings–Mack test; see the electronic supplementary material, figure S4, for histograms of distributions). Similar levels of significance were obtained for the difference in speed between $t = -300$ to $t = -50$ ms. Older fish thus use higher approach speeds and show stronger decelerations. A similar, though less pronounced, pattern is seen in the lateral

speeds (electronic supplementary material, figure S5a). Lateral speeds are related to steering movements and reduction of aim errors (electronic supplementary material, figure S5b). Both are highest for 3-day-old fish, but converge to similar values for all days at about 150–100 ms before the strike. The differences between days at –300 ms were also highly significant (Skillings–Mack, $p < 0.0001$).

Speed transients around the moment of the strike were, however, very similar (figure 3a). Independent of age, averaged forward speeds sharply increased just before the strike, and declined immediately after the strike. The sharpness of the averaged curves and small deviations relative to the means show that this pattern is highly reproducible and precisely timed for each fish, as well as between fish. Lateral speeds just before the strike, related to final directional adjustments, were very similar for different days (electronic supplementary material, figure S5a).

The differences between days in swimming speed during the approach were accompanied by clearly different patterns in mean body curvatures (figure 3b). Most strikingly, older fish, especially the 3-day-old fish used higher curvatures early on, but sharply reduced curvatures towards the strike. One-day-old fish used lower curvatures in the initial phase, but maintained relatively higher curvatures towards the moment of the strike. Mean curvatures at e.g. –300 ms were significantly different between days ($p = 0.0018$, Skillings–Mack test), as were the difference in slopes of the curvature curves ($p < 0.0001$, Skillings–Mack test for differences between $t = -300$ and $t = -50$ ms). Differences in curvatures and swimming speeds were associated with larger initial aim errors (electronic supplementary material, figure S5b) and a larger range of approach angles and distances (electronic supplementary material, figure S6). The final accelerations and directional corrections during the strike were not accompanied by substantial changes in mean body curvature. Similar to the example in figure 2, mean curvatures were low just before the moment of the strike. The more pronounced reduction of body curvature for older fish was notably accompanied by a faster reduction of aim error (electronic supplementary material, figure S5b).

Although mean body curvature changed considerably with age, pectoral fin movements, illustrated by the angle between the fins (figure 4a), modulation of abduction angle (figure 4b) and of projected fin area (figure 4c) were highly consistent. Especially, the change from alternating fin strokes during approach to synchronized strokes during and immediately after the strike was nearly identical for all days. Synchronous fin movements started with an initial adduction, leading to a sharp reduction in angle between the fins, followed by large fin abductions, to an angle well over 200° . Similar to the transients in speed, these synchronous pectoral fin movements were very precisely timed to the moment of the strike.

The angle between the fins (figure 4a) reveals the characteristic change from alternating to synchronous fin strokes, but does not adequately capture the alternating fin ad- and abductions during the approach. To quantify the modulations we performed a discrete Fourier analysis on left fin abduction and surface area for a time period from –360 to –60 ms. Figure 4b,c shows the amplitudes and frequencies of modulations for individual prey captures. The marginal histograms show that neither abduction amplitudes (GLMM: $F_{2,1748} = 1.14$, $p = 0.3190$) nor frequencies (GLMM:

$F_{2,1748} = 0.30$, $p = 0.7435$) differed significantly between ages. On average, the fish modulate abduction angles over a range of about 60° (twice the amplitude) at a frequency of about 13 Hz. Despite similarity of amplitudes and frequencies of abduction modulations, the angle between the fins during approach is larger for younger fish, indicating that they keep their fins on average at a larger abduction angle. For projected fin surface area (in a horizontal plane), we see a clear amplitude increase with age (figure 4c, upper histogram). The difference in amplitude of projected fin area modulation was highly significant (GLMM: $F_{2,1748} = 26.26$, $p < 0.0001$). Thus, 1-day-old fish modulated fin orientation (i.e. pro- and supination) only little, whereas older fish increased the modulation of fin orientation, enabling more efficient control over thrust and steering.

For all days, averaged vergence angles show a consistent, gradual increase until about 50–100 ms before the final strike (figure 5a), as required for binocular vision when distances become smaller. Vergence angles show a consistent, but counterintuitive change with age. Rather than increasing binocular overlap by increasing vergence angles the fish actually use smaller vergence angles when growing older. It should be noted that the increase in vergence while approaching prey was quite modest (maximum vergence angles about 46°) and was insufficient to stabilize the prey's image on the retina. This is illustrated in the electronic supplementary material, figure S7, which shows averaged vergence angles for all captures per day as a function of viewing distance. Especially below viewing distances of about 5–6 mm the increase of vergence while approaching was insufficient for stable fixation. Electronic supplementary material, figure S7 also shows that differences in vergence angles between days, as shown in figure 5a were larger than one should expect based on differences in viewing distance at equivalent points in time. Especially at short viewing distances, below about 5 mm, averaged vergence angles decreased with age. These differences in vergence eye movements were not accompanied by substantial differences in either version eye movements (figure 5b) or related fixation errors (electronic supplementary material, figure S5c). Version eye movements were on average quite small. Especially 3-day-old fish keep their eyes on average at a fairly constant version angle of about 2° . For all days, the fixation errors steeply declined towards a minimum of about 3.5° at 150 ms before the strike, and thereafter remained rather constant.

4. Discussion

Like many fishes, metallic livebearers ingest their prey by means of suction, generating a strong water flow into the mouth from which prey cannot escape. Owing to the steep decline of water speeds with distance from the mouth, suction feeding is only successful if the mouth approaches the prey within very short distance [24,25]. Similar to other predatory fishes, successful captures therefore require perfectly timed suction in combination with adequate swimming control in the approach phase [26,27]. Our results show how neonates of live-bearing fish are capable of capturing prey that move irregularly at substantial speeds within hours after birth, indicating that visuo-motor control is at least partly present at birth. The fish do, however, show a marked improvement in prey capture success in the first couple of days (figure 1), showing that part of the behaviour

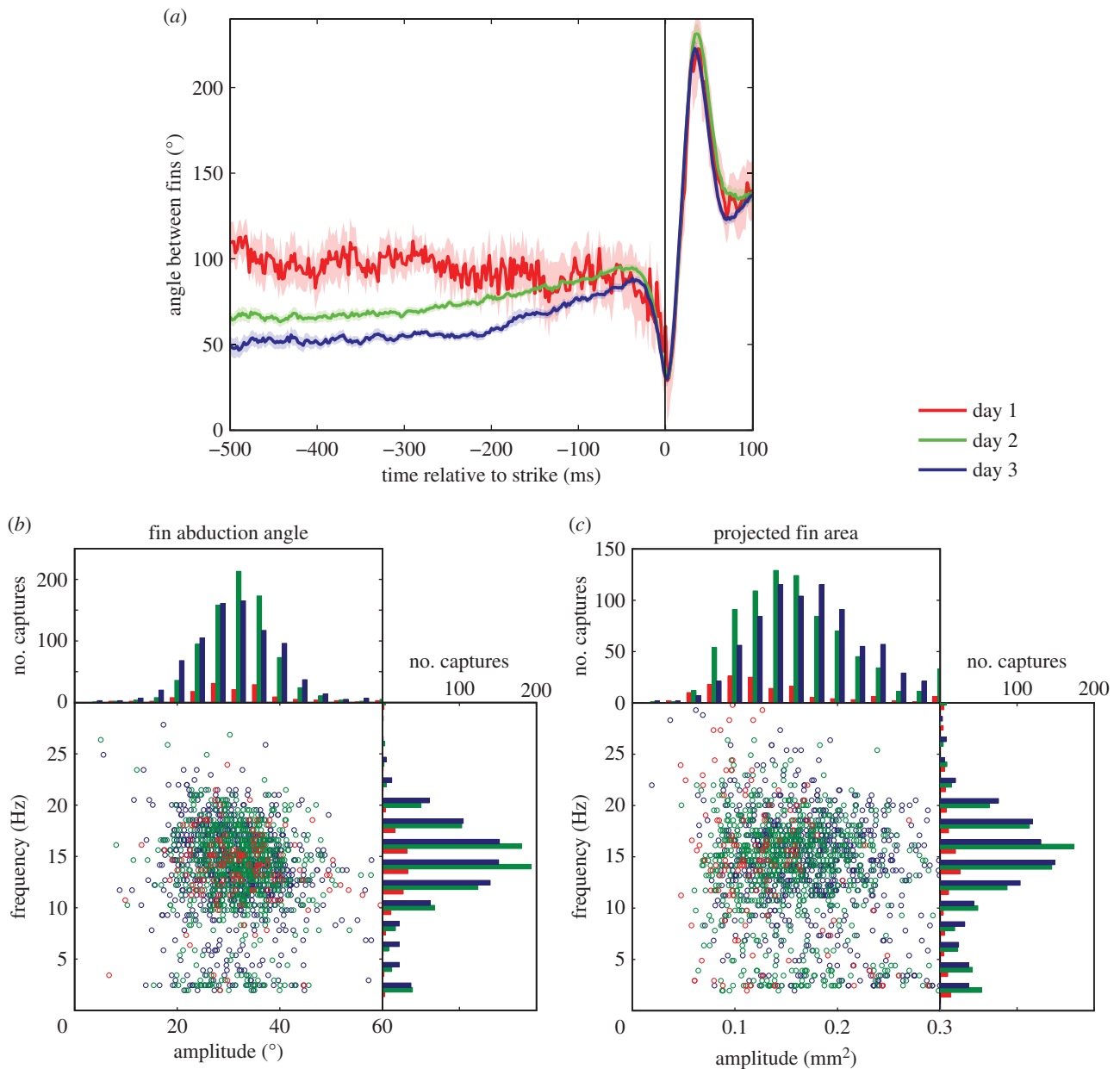


Figure 4. Pectoral fin movements during prey capture events. (a) Mean angle between the fins for days 1, 2 and 3. The format of panel (a) and the number of observations is the same as in figure 3. (b) Amplitude and frequency distributions of modulations of left fin abduction angle. (c) Amplitude and frequency distributions of temporal modulations of project fin surface area for the left fin. Each data point in the panels represents a single capture event. Modulation parameters were obtained using a discrete Fourier Transform (FFT) analysis for a time period from -360 to -60 ms relative to the moment of the strike.

also requires post-natal development. By analysing the complex coordination of eye movements, body curvatures, and pectoral fin use, we showed which parts of the behaviour are invariant with age and which aspects show changes that may correlate with improved performance.

The general strategy, involving vergence eye movements, coordinated use of both tail and pectoral fins during the approach, and the switch from alternating pectoral fin strokes during the approach to synchronous fin movements during and immediately after prey intake, was highly consistent across days. Although one cannot exclude a contribution from fast learning, the basics for this pattern seem well established at birth and are presumably to a large extent innate. This is different from e.g. zebrafish, where muscular and neuronal development of the pectoral fins is prominent in larval and in the post-larval stages [28,29]. Larval zebrafish primarily use axial musculature [30] and typical J-bends in approaching prey [8,31]. While growing up, zebrafish larvae undergo drastic

changes in swimming kinematics, associated with substantial changes in the Reynolds number [32–34]. Live-bearing fish skip the free-living larval stage and are born in an advanced juvenile stage, in which they are able to capture prey within hours. A well-developed component of prey-capturing skills that is operational immediately after birth and that is specifically adapted to the appropriate Reynolds number regime prepares the juveniles for immediate success, and supports survival through the first critical days.

In live-bearing fish, especially synchronized pectoral fin movements for prey intake and braking are well developed on the day of birth (figure 4). Use of the pectoral fins rather than tail beats allows for immediate and symmetrical steering and acceleration control owing to their bilateral position close to the centre of mass. This precludes unwanted yaw movements associated with tail fin propulsion [32,33] and supports ‘immediate’ final steering adjustments for capturing mobile prey. Moreover, the full adduction prepares the fish

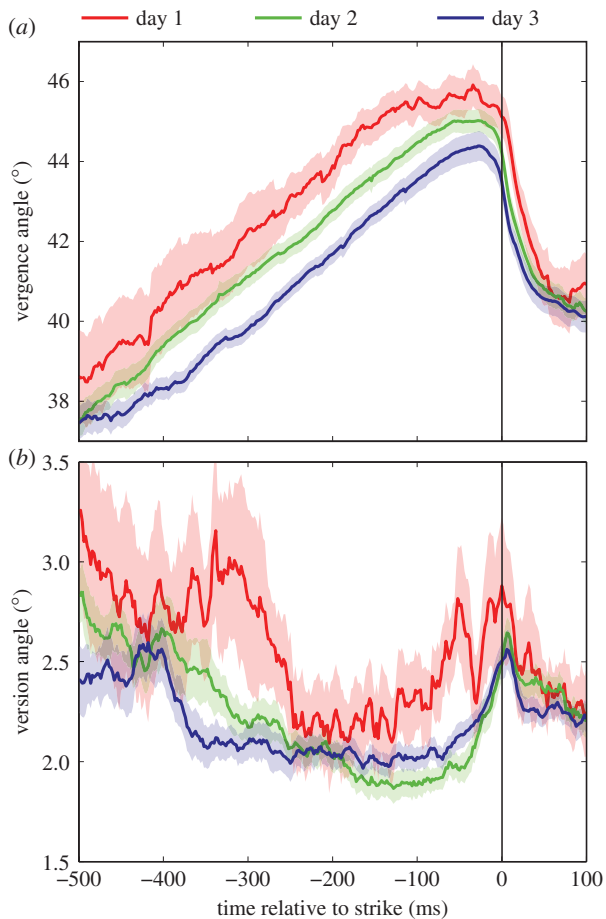


Figure 5. Vergence and version eye movements during prey capture. The format and number of measurements is the same as in figures 3 and 4a. (a) Mean vergence angles averaged for all fish. (b) Mean absolute version angles averaged for all fish.

for the post-strike brake using a large-amplitude, symmetrical abduction (figure 4a), similar to the braking manoeuvres previously observed after prey capture [31,35].

Increasing the vergence angle of the eyes upon approaching prey is also fully present at birth, emphasizing the importance of creating a binocular visual field for prey capture. Vergence movements that we observed were generally insufficient to stabilize prey images on the retinae (electronic supplementary material, figure S7). Visual localization and distance estimates therefore require localizing prey images that move across the retina, and combining this visual information with information on eye orientations. Surprisingly, the fish reduce their vergence angles when growing older, both at similar points in time (figure 4) and at similar distances from the prey (electronic supplementary material, figure S7), implying that older fish use more peripheral parts of their visual field as they approach prey. Version eye movements were generally small, especially for older fish (figure 3b), despite the largest aim errors (electronic supplementary material, figure S5b). Older fish therefore use larger variations in retinal eccentricity than newborn fish.

Although pectoral fin use for the final attack seems innate, newborn fish are limited in the use of axial musculature for agile turning and approaching prey. Older fish use higher initial curvatures, generating larger accelerations and larger angular turns, but reduce curvatures rapidly towards the strike (figure 3). At the same time, they improve pectoral fin control for aiming, by increasing axial fin rotations (figure 4c). Improvements of tail fin control coincide with

reductions in both vergence and version eye movements (figure 3), both relevant for visual coordination. This suggests postnatal development of visually guided behaviour, presumably by means of learning and calibration of visuomotor interactions. Other factors may, however, also have played a role. Although we fed fish in each session until satiation, we cannot rule out differences in motivation between days. How this would specifically affect our results remains unclear. Some effects may also partly relate to general growth or development. Growth per day was, however, limited to a few per cent (figure 1), whereas speeds changed by at least a factor of two (figure 3a). Moreover, the fish are actually capable of agile, fast starts and high-speed swimming, as illustrated by vigorous escape responses to startle stimuli immediately after birth (M. J. Lankheet 2015, unpublished data). In zebrafish, visually guided behaviour, such as the oculomotor response, visually induced escape responses and visually guided prey capture, develops in the larval stage, within days after hatching [7,12,14,16,17,36]. Live-bearing fish therefore have ample time for experience-independent development while in the uterus, but specifically lack normal perceptual-motor interactions that are supposedly required for complex tasks. Observed changes in prey capture behaviour are therefore likely to result at least partly from postnatal learning and calibration (e.g. matching visual information to motor output). Similar learning and calibration processes have been studied in zebrafish and involve predictive internal representations of visual feedback [12,18].

Because successful prey capture requires a successful approach as well as successful prey intake, our data also imply that suction feeding is operational quickly after birth. Our movies were aimed at quantifying swimming behaviour and therefore do not allow us to study details of the suction feeding mechanism, but in most cases we were able to quantify the timing of upper jaw protrusion, which is an essential part of suction feeding in metallic livebearers. These results show that protrusion is highly similar on days 1, 2 and 3. There is, however, a clear change in the timing of protrusion (see the electronic supplementary material, figure S8). These changes were significant from days 2 to 3, but non-significant from days 1 to 2. Important changes in swimming behaviour during the approach phase therefore seem to precede, at least partly, improvements in the timing of protrusion.

In live-bearing *G. metallicus*, we showed that visually guided prey capture is partly functional within hours after birth, and partly develops after birth. Tail coordination, involving predictions of forward accelerations and corresponding yaw movements for complex motor patterns was poorly developed at birth and is presumably too complex to acquire without proper sensory-motor feedback. *Girardinus metallicus* combines the development of such complex behaviour with innate control over pectoral fins to support immediate foraging success at birth.

Ethics. All animal experiments were conducted according to the standards of the ethical committee of Wageningen University (approval code 20140009).

Data accessibility. Data supporting this article are deposited in the digital Dryad repository.

Authors' contributions. All authors participated in the design of the study. T.S. carried out all measurements; M.J.L. built the experimental set-up, developed the software for data analysis, carried out the data and statistical analyses and drafted the manuscript; B.J.A.P. helped in statistical analyses and in drafting the manuscript; all authors

provided comments on drafts of the manuscript and gave final approval for publication.

Competing interests. We have no competing interest.

Funding. This experiment received no funding from grants.

Acknowledgements. We are very grateful to Henk Schipper and Remco Pieters for technical assistance and to the staff of the CARUS animal housing facility for excellent support in taking care of experimental animals.

References

- Starck JM, Ricklefs RE. 1998 *Avian growth and development—evolution within the altricial–precocial spectrum*. Oxford, UK: Oxford University Press.
- Derrickson EM. 1992 Comparative reproductive strategies of altricial and precocial mammals. *Funct. Ecol.* **6**, 57–65. (doi:10.2307/2389771)
- Dial KP, Jackson BE. 2011 When hatchlings outperform adults: locomotor development in Australian brush turkeys (*Alectura lathami*, Galliformes). *Proc. R. Soc. B* **278**, 1610–1616. (doi:10.1098/rspb.2010.1984)
- Balon EK. 1981 Saltatory processes and altricial to precocial forms in the ontogeny of fishes. *Am. Zool.* **21**, 573–596. (doi:10.1093/icb/21.2.573)
- Pollux BJA, Meredith RW, Springer MS, Garland T, Reznick DN. 2014 The evolution of the placenta drives a shift in sexual selection in livebearing fish. *Nature* **513**, 233–236. (doi:10.1038/nature13451)
- Reznick DN, Mateos M, Springer MS. 2002 Independent origins and rapid evolution of the placenta in the fish genus *Poeciliopsis*. *Science* **298**, 1018–1020. (doi:10.1126/science.1076018)
- Bianco IH, Kampff AR, Engert F. 2011 Prey capture behavior evoked by simple visual stimuli in larval zebrafish. *Front. Syst. Neurosci.* **5**, 101. (doi:10.3389/fnsys.2011.00101)
- Borla MA, Palecek B, Budick S, O'Malley DM. 2002 Prey capture by larval zebrafish: evidence for fine axial motor control. *Brain Behav. Evol.* **60**, 207–229. (doi:10.1159/000066699)
- Budick SA, O'Malley DM. 2000 Locomotor repertoire of the larval zebrafish: swimming, turning and prey capture. *J. Exp. Biol.* **203**, 2565–2579.
- Fero K, Yokogawa T, Burgess HA. 2011 The behavioral repertoire of larval zebrafish. In *Zebrafish models in neurobehavioral research*, vol. 52, *Neuromethods* (eds A Kaluff, JM Cachat), pp. 249–291. New York, NY: Humana Press.
- Orger MB, Kampff AR, Severi KE, Bollmann JH, Engert F. 2008 Control of visually guided behavior by distinct populations of spinal projection neurons. *Nat. Neurosci.* **11**, 327–333. (doi:10.1038/nn2048)
- Portugues R, Engert F. 2011 Adaptive locomotor behavior in larval zebrafish. *Front. Syst. Neurosci.* **5**, 72. (doi:10.3389/fnsys.2011.00072)
- Trivedi CA, Bollmann JH. 2013 Visually driven chaining of elementary swim patterns into a goal-directed motor sequence: a virtual reality study of zebrafish prey capture. *Front. Neural Circuits* **7**, 86. (doi:10.3389/fncir.2013.00086)
- Semmelhack JL, Donovan JC, Thiele TR, Kuehn E, Laurrell E, Baier H. 2014 A dedicated visual pathway for prey detection in larval zebrafish. *Elife* **3**, e04878. (doi:10.7554/eLife.04878)
- Beck JC, Gilland E, Tank DW, Baker R. 2004 Quantifying the ontogeny of optokinetic and vestibuloocular behaviors in zebrafish, medaka, and goldfish. *J. Neurophysiol.* **92**, 3546–3561. (doi:10.1152/jn.00311.2004)
- Easter SSJr, Nicola GN. 1996 The development of vision in the zebrafish (*Danio rerio*). *Dev. Biol.* **180**, 646–663. (doi:10.1006/dbio.1996.0335)
- Easter SSJr, Nicola GN. 1997 The development of eye movements in the zebrafish (*Danio rerio*). *Dev. Psychobiol.* **31**, 267–276. (doi:10.1002/(SICI)1098-2302(199712)31:4<267::AID-DEV4>3.0.CO;2-P)
- Portugues R, Feierstein CE, Engert F, Orger MB. 2014 Whole-brain activity maps reveal stereotyped, distributed networks for visuomotor behavior. *Neuron* **81**, 1328–1343. (doi:10.1016/j.neuron.2014.01.019)
- Severi KE, Portugues R, Marques JC, O'Malley DM, Orger MB, Engert F. 2014 Neural control and modulation of swimming speed in the larval zebrafish. *Neuron* **83**, 692–707. (doi:10.1016/j.neuron.2014.06.032)
- Stewart WJ, Cardenas GS, McHenry MJ. 2013 Zebrafish larvae evade predators by sensing water flow. *J. Exp. Biol.* **216**, 388–398. (doi:10.1242/jeb.072751)
- Howard IP, Rogers BJ. 1995 *Binocular vision and stereopsis*. Oxford, NY: Oxford University Press.
- Littell RC, Henry PR, Ammerman CB. 1998 Statistical analysis of repeated measures data using SAS procedures. *J. Anim. Sci.* **76**, 1216–1231.
- Skills JH, Mack GA. 1981 On the use of a Friedman-type statistic in balanced and unbalanced block designs. *Technometrics* **23**, 171–177. (doi:10.1080/00401706.1981.10486261)
- van Leeuwen JL, Muller M. 1984 Optimum sucking techniques for predatory fish. *Trans. Zool. Soc. Lond.* **37**, 137–169. (doi:10.1111/j.1096-3642.1984.tb00069.x)
- Wainwright PC, McGee MD, Longo SJ, Hernandez LP. 2015 Origins, innovations, and diversification of suction feeding in vertebrates. *Integr. Comp. Biol.* **55**, 134–145. (doi:10.1093/icb/icv026)
- Kane EA, Higham TE. 2011 The integration of locomotion and prey capture in divergent cottid fishes: functional disparity despite morphological similarity. *J. Exp. Biol.* **214**, 1092–1099. (doi:10.1242/jeb.052068)
- Longo SJ, McGee MD, Oufiero CE, Waltzek TB, Wainwright PC. 2016 Body ram, not suction, is the primary axis of suction-feeding diversity in spiny-rayed fishes. *J. Exp. Biol.* **219**, 119–128. (doi:10.1242/jeb.129015)
- Thorsen DH, Hale ME. 2005 Development of zebrafish (*Danio rerio*) pectoral fin musculature. *J. Morphol.* **266**, 241–255. (doi:10.1002/jmor.10374)
- Thorsen DH, Hale ME. 2007 Neural development of the zebrafish (*Danio rerio*) pectoral fin. *J. Comp. Neurol.* **504**, 168–184. (doi:10.1002/cne.21425)
- Hale ME. 2014 Developmental change in the function of movement systems: transition of the pectoral fins between respiratory and locomotor roles in zebrafish. *Integr. Comp. Biol.* **54**, 238–249. (doi:10.1093/icb/ict014)
- McClenahan P, Troup M, Scott EK. 2012 Fin-tail coordination during escape and predatory behavior in larval zebrafish. *PLoS ONE* **7**, e32295. (doi:10.1371/journal.pone.0032295)
- Li G, Müller UK, van Leeuwen JL, Liu H. 2012 Body dynamics and hydrodynamics of swimming fish larvae: a computational study. *J. Exp. Biol.* **215**, 4015–4033. (doi:10.1242/jeb.071837)
- Müller UK, van den Boogaart JGM, van Leeuwen JL. 2008 Flow patterns of larval fish: undulatory swimming in the intermediate flow regime. *J. Exp. Biol.* **211**, 196–205. (doi:10.1242/jeb.005629)
- van Leeuwen JL, Voeseck CJ, Müller UK. 2015 How body torque and Strouhal number change with swimming speed and developmental stage in larval zebrafish. *J. R. Soc. Interface* **12**, 20150479. (doi:10.1098/rsif.2015.0479)
- Higham TE. 2007 Feeding, fins and braking maneuvers: locomotion during prey capture in centrarchid fishes. *J. Exp. Biol.* **210**, 107–117. (doi:10.1242/jeb.02634)
- McElligott MB, O'Malley DM. 2005 Prey tracking by larval zebrafish: axial kinematics and visual control. *Brain Behav. Evol.* **66**, 177–196. (doi:10.1159/000087158)